Chris Acott

No. We do not really know what is actually happening when we treat patients. What we are arguing about is that perhaps recovery might be neuronal recruitment. If so, divers are knocking off their neuronal reserves with each attack of DCI.

Dr C J Acott FANZCA, DipDHM, is the Co-ordinator of the Diving Incident Monitoring Study (DIMS) and a consultant for the Diver Emergency Service. His address is Hyperbaric Medicine Unit, Department of Anaesthesia and Intensive Care, Royal Adelaide Hospital, North Terrace, Adelaide, South Australia 5000, Australia. Phone +61-8-8222-5116. Fax +61-8-8232-4207

UNCERTAINTIES IN PREDICTING DECOMPRESSION ILLNESS

David Doolette

Key Words

Bubbles, decompression illness, physiology, research.

Introduction

Decompression tables present a list of ostensibly safe schedules. Divers may expect that dives conducted according to such schedules will be free from decompression illness (DCI) and dives outside the limits will result in DCI. This belief is embodied in Haldane's statement, subsequent to the publication of his decompression tables, "that compressed-air illness has now practically disappeared except in isolated cases where from one cause or another the regulations have not been carried out".[1] The basis for this misconception might be the classification of diving outcome into DCI or no DCI. Using this classification, a particular dive either will or will not result in DCI for an individual. However, the outcome of an identical dive profile may differ for another individual, or the same individual on another occasion. The categorical assertion that decompression schedules distinguish safe (zero risk of DCI) from unsafe dives for the entire population is not only untrue but also impossible. Many commonly used decompression tables have a reasonably low risk of DCI, but any assumption of safety obscures the fact that there will be exceptional incidents of DCI.

Despite his later unequivocal statement, Haldane's original work with goats showed typical biological variability in individual animal susceptibility to DCI.[2] Figure 1 shows some of Haldane's goat data plotted in the form of a dose–response curve. This curve illustrates a low, but finite risk of DCI, following a trivial diving exposure (in this case low exposure pressure) with the risk increasing with the exposure. The exposure where risk rises most rapidly defines the most common limiting exposure for the population. Haldane's (and all subsequent) assertion of safety is based on defining the limiting exposure from a point towards the left of this curve. However, theoretically, there is no point on such dose–response curves where risk is zero.

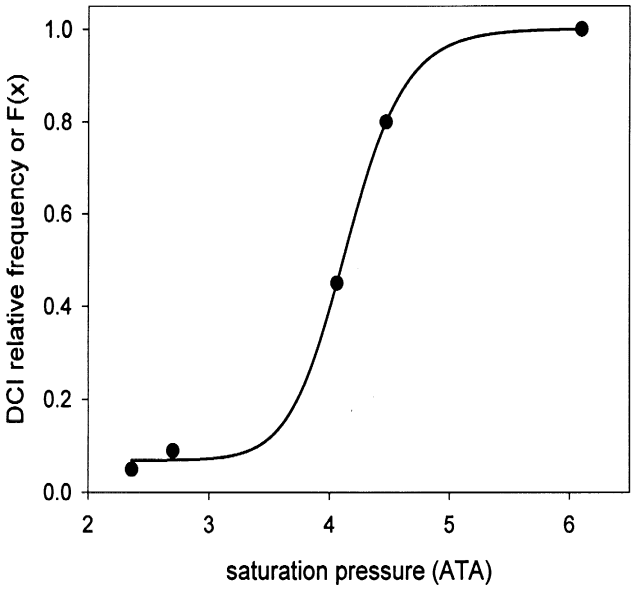

Figure 1. Dose–response curve (cumulative distribution function) for DCI constructed from data tabulated in Haldane's experimental studies with goats.[2] Groups of 4 to 23 goats were exposed to the pressure indicated on the x-axis for 4 hours (3 hours at 4.47 ATA) and decompressed to 1 ATA over 2 to 10 minutes (31 minutes from 6.1 ATA). The circles show the proportion (relative frequency) of goats experiencing any symptoms of DCI. The line is a sigmoid curve, F(x), fitted to the original data.

This paper examines two aspects of uncertainty involved in the prediction of DCI. Firstly, DCI is the result of complex processes that are only superficially evaluated in the decompression theory that underlies decompression tables. Secondly, the main aim is to illustrate that sensitivity to DCI will be normally distributed in a population of divers.

The normal distribution

The sigmoid dose-response curve in figure 1 is derived from an underlying bell-shaped distribution of sensitivity to DCI (see Figure 2). Many biological phenomena conform to a particular bell-shaped distribution called the "normal distribution".

Figure 3 that shows computer simulations of 3 different dice experiments. The distribution of values found

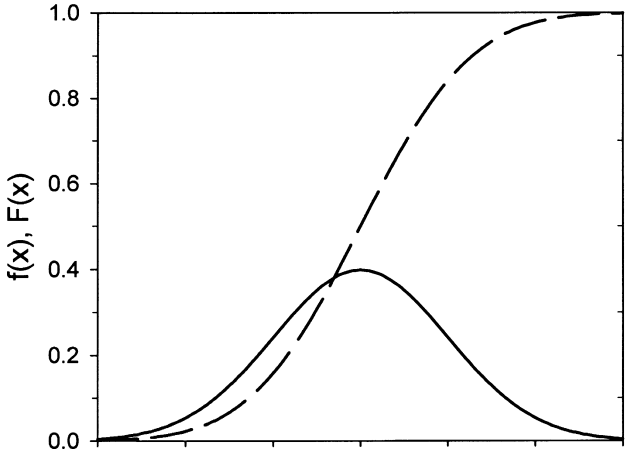

Figure 2. The normal distribution of possible values of a variable X. The x-axis gives the possible values of X. The solid line shows the normal probability density function, f(x) and the dashed line shows the cumulative density function, F(x).

for a sample of 1,000 rolls of one die is shown in figure 3a. If the die is fair, each value from 1 to 6 is equally likely (rectangular or uniform probability distribution function) and this is reflected in the frequency distribution. However the sum of two dice rolled 1,000 times, shown in figure 3b, shows more results in the centre because there is only one way to get a sum of 2 or of 12 but six ways to get a sum of 7. Overlaid on this frequency distribution is the predicted normal probability density function (normal distribution). Figure 3c shows the frequency distribution of the sum of 100 dice rolled simultaneously and repeated 1,000 times. The levels of observed sums are on the x-axis (intervals of 5) and the bars represent the frequencies of those sums (y-axis). Sums near 350 are common and larger or smaller levels are increasingly less common. The frequency distribution is clearly normally distributed, fitting the bell shaped curve of the predicted normal probability density function. This is a (idealised) mathematical model of the frequency distribution. Whereas the probability density is an abstract concept, this continuous function can be seen as describing the *relative* frequency for *every* level on the x-axis (even though only integer levels are possible in the case of dice sums).

The probability (numerically equivalent to the relative frequency) of an individual event in a population can be estimated from the probability density function of a sample. For example, in the dice experiment of figure 3c, only sums between 295 and 417 occurred in this sample of 1,000 rolls, although sums between 100 and 600 are possible. Using the normal probability density function the probability of rolling any number, say 590 (which would be very low), can be estimated. The probability of any range of levels is estimated from the area under the probability density function (integral) over that range. The cumulative distribution function (or probability integral) gives the probability of all levels less than or equal to each value on the x-axis. For a bell-shaped curves the cumulative

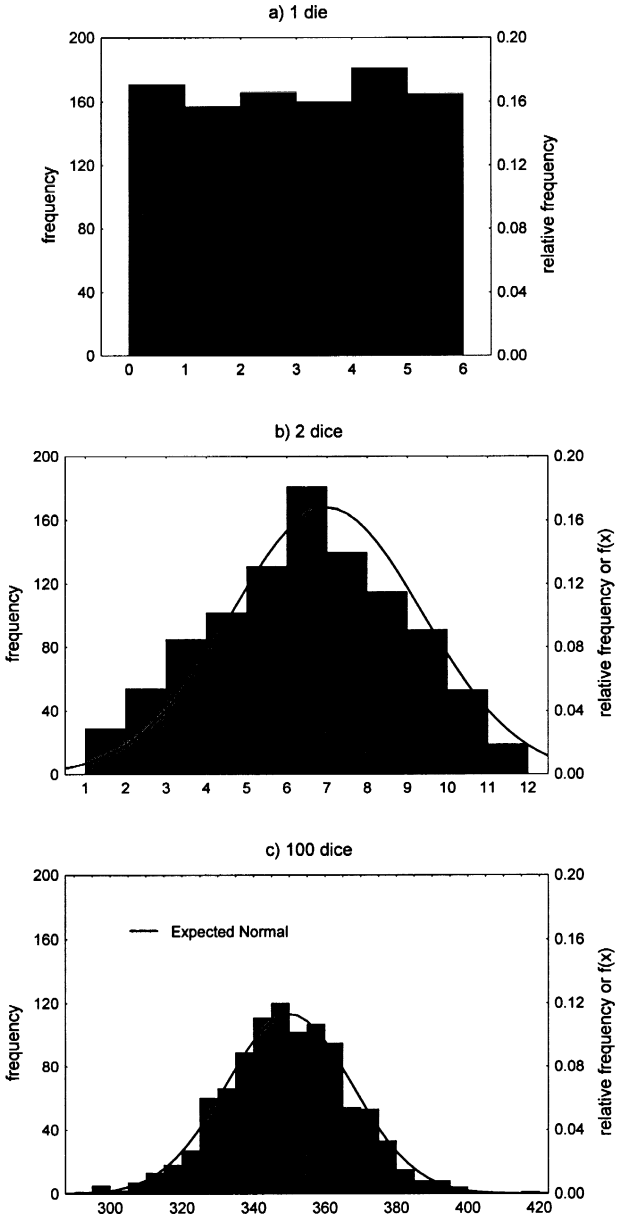

Figure 3. Frequency histograms of a computer simulation of dice rolling experiments illustrating the central limit theorum. The histograms are of the frequency and relative frequency (y-axis) of the sum of the face values (x-axis). The simulations are for 1,000 rolls of 1 (3a), 2 (3b) or 100 (3c) dice. Overlaid on histograms 3b and 3c is the predicted normal probability distribution function (solid line), f(x).

distribution function is sigmoid (see figure 2). For the dice experiment the cumulative distribution function at 590 would estimate the probability of rolling 590 or less (which would be very high).

The normal probability density function describes a family of symmetrical bell-shaped curves that differ only in height and width. The height and width of the curve is determined by a single parameter, the standard deviation.

A quite different experiment could result in a frequency distribution with a similar appearance. The risk of DCI for an upward excursion from saturation is a function of the decompression and the time spent at reduced pressure.

If a group of subjects were decompressed, a frequency histogram of the number of individuals first displaying symptoms (y-axis) during various time intervals (x-axis) might look like the histogram in figure 3c and could be described using a normal probability density function. In other words the sensitivity to DCI in this sample would be normally distributed. If the cumulative number of individuals having displayed symptoms at each time interval was plotted against the same x-axis the result could be described using cumulative distribution function. Such a cumulative distribution function is recognisable as a dose–response curve where the value at any time would estimate the probability of DCI for an individual exposed to that pressure for that duration.

Although the results of many experimental designs naturally present as sigmoid dose–response curves (cumulative distribution function) the underlying bell-shaped probability distribution is not obvious. A common experimental design is to expose groups of subjects to different levels of decompression stress (e.g. exposure pressure, exposure time, extent of decompression) and record the number of individuals from each group displaying symptoms of DCI. A plot of the relative frequency of symptoms in each group (y-axis) against decompression stress (x-axis) would give a sigmoid dose–response curve as is shown in Figure 1 using some of Haldane's original data.

An important aspect of probability density functions is the belief that a relatively few models (of which the normal probability density function is an important one) fit many real world situations, a notion supported by empirical observation. Many biological phenomena appear to be normally distributed which can be in part explained by the central limit theorem.

Central Limit theorem

A simplified explanation of this theorem states that, given certain conditions, if a variable (S_n) is the result of a sum of a large number of other variables ($S_n=X_1+X_2+\ldots+X_n$), a sample of variable S_n will be normally distributed.

This is true regardless of how the underlying variable (X_1, X_2,…X_n) are distributed. This is illustrated in figure 3. Normal distribution is the assumed model for biological phenomena because any measured variable (e.g. sensitivity to DCI) is the result of many underlying genetic and environmental factors.

A biological response as complicated as DCI is the result of many contributing factors, ranging from the well quantified to the unknown. By virtue of the central limit theorem alone, it is reasonable to predict that sensitivity to DCI should be normally distributed in a population and therefore outcome after decompression is uncertain. To illustrate that this is not just a statistical "black-box" approach, we will now examine experimental findings of aspects of the cascade of events that lead to DCI to see if they conform to this prediction of a normal distribution.

Events leading to DCI

For any dive, the sequence of events leading to DCI can be grouped broadly into:

1 uptake and elimination of inert gas;
2 bubble formation upon decompression; and
3 pathophysiological response to bubbles.

Decompression schedules determine the presence or absence of DCI following any defined dive profile (pressure/time/breathing gas history) using mathematical models incorporating some or all of these mechanisms. In typical decompression models, the input (dive profile) and output (DCI) are measured but the intervening mechanisms are modelled using latent variables (unobserved theoretical constructs). In other words, the models are not based on actual measurements of tissue gas uptake or bubble formation. Haldane's schedules, and later derivations, calculate uptake and elimination of inert gas (latent variable) in the context of a threshold for symptoms of DCI, with only the implicit assumption that bubbles do not form within safe schedules.[2] Later models have incorporated bubble formation as a latent variable with varying degrees of sophistication.[3] Most models do not incorporate pathophysiological responses.

Uptake and elimination of inert gas

Mathematical models of inert gas kinetics come in varying degrees of sophistication. Distributed models account for diffusion of gas between capillaries and tissue units of specified geometry. The membrane-limited diffusion compartmental model ignores tissue geometry and confines diffusion to a membrane between well-stirred blood and tissue compartments. The simplest model is the single perfusion limited compartment, which ignores tissue geometry and diffusion, where gas uptake into a well-stirred compartment, consisting of tissue and blood, is limited only by delivery of gas in the arterial blood. Each simplification results in a more easily handled set of equations. The difference between arterial blood and a single perfusion limited compartment gas content declines exponentially with a rate constant, defined by blood flow, compartment volume and solubility of gas in blood and tissue. Many decompression models incorporate several theoretical well-

stirred single perfusion limited compartments that are not identified with any particular body tissue. It is unfortunate that a misleading interchange of the terms compartment and tissue is found in decompression literature. As this is a theoretical treatment, actual inert gas content of any identified critical tissues is never known. In fact, perfusion limited models have been shown to fit poorly to actual gas exchange data.[4]

Nevertheless, even the most sophisticated deterministic model will not account for the distribution of inert gas uptake across individuals. Figure 4 shows the frequency distribution of concentration of inert gas tracer (nitrous oxide) in the brains of 9 sheep after 15 minutes inhalation of that gas under similar conditions. A distribution with a wide dispersion and some central tendency is identifiable even in this small sample. The predicted normal probability density function is overlaid on the histogram. Statistical analysis (Shapiro-Wilks W test) indicates that this sample is normally distributed.

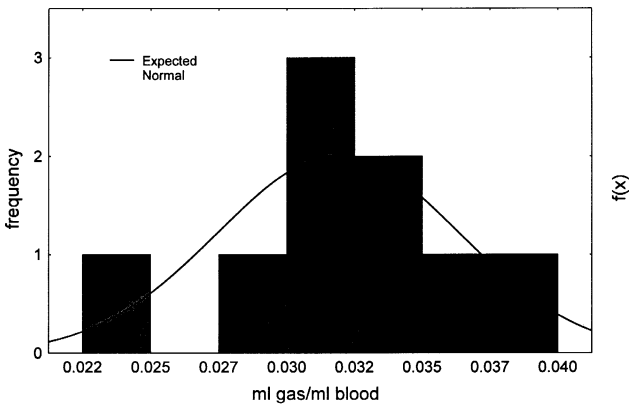

Figure 4. Frequency distribution of inert gas (nitrous oxide) concentration in sheep brain. Nine sheep breathed 10% nitrous oxide for 15 minutes and nitrous oxide content of brain effluent blood was assayed by headspace gas chromatography. Values of brain effluent inert gas concentrations are on the x-axis and the frequency of those values on the y-axis. The solid line is the predicted normal probability distribution function, f(x).

Bubble formation

Bubbles form in tissues if ambient pressure is reduced below total tissue dissolved gas tension (concentration/solubility). Bubble formation is important for two reasons, both dependent on the total amount of gas that separates into bubbles. Firstly, bubbles probably cause DCI. Secondly, elimination of gas from tissue containing free (undissolved) gas (bubbles) will be slower than predicted by many decompression models. The peak volume of free gas that separates from tissue depends on the number of bubbles.[5] The number of bubbles that form for any given decompression is difficult to predict. If bubble inception can result from homogenous nucleation, the rate of bubble number formation will be critically dependent on the surface tension at the site of bubble formation, which is unknown. If, as is widely believed, bubbles nucleation is heterogeneous, the number (and distribution) of these pre-existing nuclei must also be known.

It is difficult to find data on number of nuclei except in the engineering cavitation literature. Figure 5 shows some of the data of Crump of bubble formation from nuclei in a venturi nozzle.[6,7] Replotting the original data as a frequency distribution reveals that, under the controlled experimental conditions, the number of bubbles formed follows a normal distribution (Shapiro-Wilks W test).

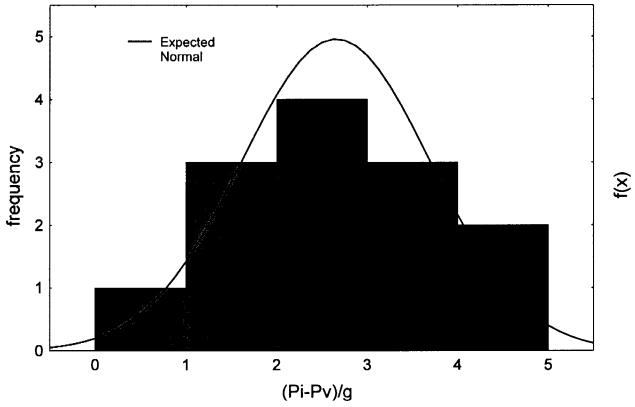

Figure 5. Frequency distribution of bubble nuclei, formed at a venturi nozzzle, in water. The histogram is constructed from data of Crump[7] shown in figure 3.2 of Knapp et al.[6] The solid line is the predicted normal probability distribution function, f(x).

Pathophysiology

DCI is a multi-causal disease and one postulated mechanism is complement activation at the blood-bubble interface. The extent of such activation will depend on the surface area of the gas phase, which will be a function of both total free gas volume and bubble number. Figure 6 shows data on the activation of C5A in blood samples with introduction of a gas stream.[8] The data for 36 such measurements (6 blood samples from each of 6 human subjects) is replotted in the form of a frequency histogram. The data is normally distributed (Shapiro-Wilks W test).

Predicting the distribution of DCI

If the processes that combine to cause DCI are each normally distributed, it is possible to predict the distribution of DCI itself. Although only a portion of all contributing factors, the uptake and elimination of inert gas, bubble formation upon decompression and the pathophysiological response to bubbles serve as examples. For any defined dive profile, the most likely level of response at each of these steps is determined by the input

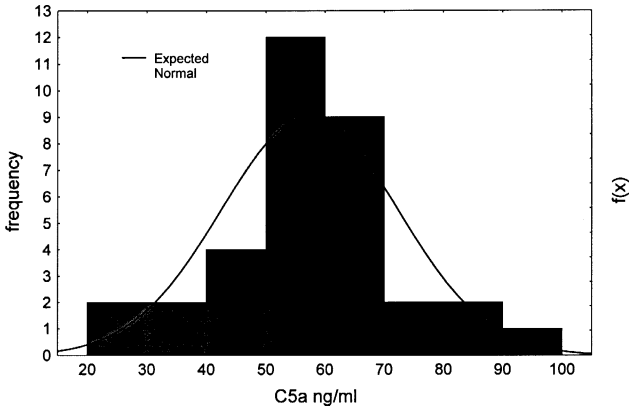

Figure 6. Frequency distribution of bubble-activated C5a in human serum. The histogram is constructed from data shown in figure 4b of Bergh et al. The solid line is the predicted normal probability distribution function, f(x).

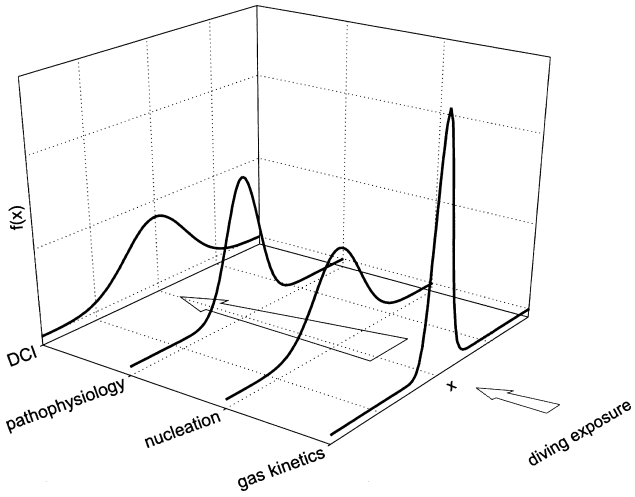

Figure 7. A linear (sequential) combination of independent normal variables has a normal distribution. The steps involved in the production of DCI are normally distributed. A process of multiplication connects the steps. As a result, DCI has a normal distribution that can be predicted from the distributions of the preceding steps.

from the preceding step. However, the input from the preceding step will not influence the shape of the distribution or determine the exact outcome of the subsequent step. Thus DCI (X_{DCI}) is the result of a linear combination of statistically independent variables (X_{GAS}, X_{BUB}, X_{PATH}). Any linear combination of independent normal variables will have a predictable normal distribution.

The standard deviation (which determines the shape) of the resulting normal probability density function can be calculated from the standard deviation of the underlying variables. The formula for this calculation depends on the nature of the linear relationship of the variables. In the current example it is reasonable to assume that a process of multiplication connects each of the events leading to DCI.

$$X_{DCI} = X_{GAS} \times X_{BUB} \times X_{PATH}$$

The coefficient of variation (CV = standard deviation/mean) allows comparison between distributions of variables with different units of measurement. For the relationship above, the coefficient of variation of DCI can be computed from the individual coefficients of variation at each step according to the following formula:[9]

$$(CV_{DCI})^2 \cong (CV_{GAS})^2 + (CV_{BUB})^2 + (CV_{PATH})^2$$

From the distributions shown in figures 4–6, CV_{GAS} = 0.14, CV_{BUB} = 0.39, and CV_{PATH} = 0.26. Using the formula above results in CV_{DCI} = 0.49. The dispersion in each intervening step combines and produces a greater dispersion in the resulting distribution. This relationship is illustrated in figure 7.

Discussion

All mathematical models are a necessary simplification of reality, but such simplification can result in inaccuracy. Decompression models present a theoretical framework for organising decompression experience, not an accurate description of the physiological and pathophysiological pathways to DCI. For instance, Haldane's experimental observations were the "safe" decompression of goats from assumed (but probably incomplete) saturation; all other aspects of his model were purely theoretical.[2] Tabulated decompression schedules may be considerably altered from the underlying model output as a result of field testing, and at the other extreme schedules generated from desktop or diver carried computer are purely model based. In the latter case the accuracy of the model is critical.

Since the sensitivity to DCI is normally distributed in a population of individuals we cannot predict a schedule that separates dives always free of DCI from those always resulting in DCI (square cumulative distribution function). Even the most sophisticated or accurate deterministic model will fail occasionally. Probabilistic decompression models attempt to address this by assigning a probability of DCI to a defined dive profile (based on mechanistic models).[10,11] Setting limits far to the left of the true sigmoid cumulative distribution function separates dives with very low risk of DCI from all others. Such conservative limits result in uselessly short bottom times. Practical schedules are a compromise between useful bottom time and acceptable risk of DCI.

The normal distribution of sensitivity to DCI does not imply that attempts to improve prediction of DCI should be abandoned. If more is learnt about the nature of the intervening processes and incorporated into more accurate models we can make better predictions of the most likely

outcome (without influencing the shape of the distribution of X_{DCI}). Such knowledge may also allow tailoring of schedules to specific populations so that the intervening normal distributions of processes would be more compact as would the final distribution of sensitivity to DCI (for that population).

References

1 Haldane JS and Priestly JG. *Respiration. 2nd ed.* Oxford: Clarendon Press, 1935

2 Boycott AE, Damant GCC and Haldane JS. The prevention of compressed-air illness. *J Hyg (Camb)* 1908; 8: 342-443

3 Hills BA. *Decompression Sickness Volume 1: The biophysical basis of prevention and treatment*. Chichester: John Wiley & Sons; 1977

4 Doolette DJ, Upton RN and Grant C. Diffusion limited, but not perfusion limited, compartmental models describe cerebral nitrous oxide kinetics at both high and low cerebral blood flows. *J Pharmacokinet Biopharm* 1998; 26: 649-672

5 Van Liew HD and Burkard ME. Density of decompression bubbles and competition for gas among bubbles, tissue, and blood. *J Appl Physiol* 1993; 75: 2293-2301

6 Knapp RT, Daily JW and Hammitt FG. *Cavitation*. New York: McGraw-Hill, 1970

7 Crump SF. *Determination of critical pressures for inception of cavitation in fresh water and sea water as influenced by air content of the water. David W. Taylor Model Basin Report No.: 575.* Washington DC: Navy Department, 1949

8 Bergh K, Hjelde A, Iversen OJ and Brubakk AO. Variability over time of complement activation induced by air bubbles in human and rabbit sera. *J Appl Physiol* 1993; 74: 1811-1815

9 Hald A. *Statistical theory with engineering applications*. New York: Chapman and Hall, 1952

10 Thalmann ED, Parker EC, Survanshi SS and Weathersby PK. Improved probabilistic decompression model risk predictions using linear-exponential kinetics. *Undersea Hyperb Med* 1997; 24: 255-274

11 Gerth WA and Vann RD. Probabilistic gas and bubble dynamics models of decompression sickness occurrence in air and N2-O2 diving. *Undersea Hyperb Med* 1997 ; 24: 275-292

David J Doolette, PhD, is a physiologist attached to the Department of Anaesthesia and Intensive Care, University of Adelaide, Adelaide, South Australia 5005. Phone +61-(0)8-8303-6382. Fax +61-(0)8-8303-3909. E-mail <ddoolett@medicine.adelaide.edu.au>.

THE NATURAL PROGRESSION OF DECOMPRESSION ILLNESS AND DEVELOPMENT OF RECOMPRESSION PROCEDURES

Richard Moon

Key Words

Decompression illness, history, treatment.

Beginnings

Whereas diving with an open bell, and hence exposure to compressed gas, dates back to at least the 16th century, when decompression illness was first observed is not known. However, when the vacuum pump was invented in the 17th century, there was a tremendous fascination with the effects of vacuum on living things. The first example of decompression illness (DCI) and subsequent recompression was described by Robert Boyle in 1670, when he described the effects on animals of decompression in a bell jar. An excerpt from one of his papers is reproduced below:

> "We took a viper and including her in the greatest sort of small receivers, we emptied the glass very carefully, and the viper moved up and down, as if it were to seek for air, and after a while, foamed a little at the mouth, and left off that foam sticking to the inside of the glass: her body swelled not considerably, and her neck less, till a pretty while after we had left pumping; but afterwards the body and neck grew prodigiously tumid and a blister appeared on the back…The jaws remained mightily opened, and somewhat distorted…the air being readmitted after 23 hours in all, the viper's mouth was presently closed, though soon after it was opened again, and continued long so; and scorching or pinching the tail made a motion in the whole body, that argued some life".

This is probably the first written account of decompression sickness (DCS) in animals (and the partial effectiveness of recompression).[1]

Compressed Air Work and Diving

The observations of Robert Boyle remained a laboratory curiosity, with little practical relevance until the development of diving and compressed air work in the 19th century. In 1854 Pol and Watelle first described DCI in miners working in compressed air at Avaleresse-la-Naville in France.[2] A compressed air environment (caisson) in which men performed the excavation, was utilised to keep water and mud out of the working environment. At that site there were 64 men employed, of whom 16 are known to have suffered accidents, and there were two deaths.